

# Partial Derivative–Based Sensitivity Analysis of Models Describing Target-Mediated Drug Disposition

Submitted: March 14, 2007; Accepted: May 3, 2007; Published: June 8, 2007

Anson K. Abraham,<sup>1</sup> Wojciech Krzyzanski,<sup>1</sup> and Donald E. Mager<sup>1</sup>

<sup>1</sup>Department of Pharmaceutical Sciences, University at Buffalo, State University of New York, Amherst, NY 14260

## ABSTRACT

Sensitivity analysis is commonly used to characterize the effects of parameter perturbations on model output. One use for the approach is the optimization of an experimental design enabling estimation of model parameters with improved accuracy. The primary objective of this study is to conduct a sensitivity analysis of selected target-mediated pharmacokinetic models, ascertain the effect of parameter variations on model predictions, and identify influential model parameters. One linear model (Model 1, control) and 2 target-mediated models (Models 2 and 3) were evaluated over a range of dose levels. Simulations were conducted with model parameters being perturbed at the higher and lower ends from literature mean values. Profiles of free plasma drug concentrations and their partial derivatives with respect to each parameter vs time were analyzed. Perturbations resulted in altered outputs, the extent of which reflected parameter influence. The model outputs were highly sensitive to perturbations of linear disposition parameters in all 3 models. The equilibrium dissociation constant ( $K_D$ ) was less influential in Model 2 but was influential in the terminal phase in Model 3, highlighting the role of  $K_D$  in this region. An equation for Model 3 in support of the result for  $K_D$  was derived. Changes in the initial receptor concentration [ $R_{tot}(0)$ ] paralleled the observed effects of initial plasma volume ( $V_c$ ) perturbations, with increased influence at higher values. Model 3 was also sensitive to the rates of receptor degradation and internalization. These results suggest that informed sampling may be essential to accurately estimate influential parameters of target-mediated models.

**KEYWORDS:** Nonlinear pharmacokinetics, quasi-equilibrium models, equilibrium dissociation constant, receptor internalization

## INTRODUCTION

Dose-dependent pharmacokinetic parameters are a hallmark of target-mediated drug disposition (TMDD), where the interaction between a drug and its pharmacological target

influences the time course of plasma concentration-time profiles.<sup>1</sup> Drugs that exhibit this phenomenon generally show a decreasing volume of distribution with increasing dose levels, and nonlinear clearance also may result if binding to the target is involved in a major elimination pathway (eg, receptor-mediated endocytosis). A general pharmacokinetic model of TMDD has been developed, where these nonlinear properties manifest from the formation and disposition of the drug-target complex.<sup>2</sup> This systematic approach has shown utility in characterizing the complex nonlinear pharmacokinetics of several small-molecule and peptide-based drugs.<sup>3</sup>

One challenge to applying the general TMDD model is the estimation of the drug–target binding constants of association and dissociation ( $k_{on}$  and  $k_{off}$ ) from in vivo pharmacokinetic data. Formation of the drug-target complex is relatively rapid with respect to kinetics, and common blood sampling schemes make it difficult or impossible to estimate these parameters for most drugs. Although various techniques may be applied to limit parameter space, a quasi-equilibrium solution of the general model has been derived that replaces the binding microconstants with the equilibrium dissociation constant ( $K_D = k_{off}/k_{on}$ ).<sup>4</sup> The quasi-equilibrium model (QEM) was applied to leukemia inhibitory factor (LIF) pharmacokinetic data in sheep; these data had been characterized previously using the TMDD model.<sup>5</sup> Predicted concentration-time profiles appeared to be identical in the 2 models, and there was good agreement in parameter estimates, with the exception of the  $K_D$  term. Although several explanations might exist, it was hypothesized that the model may be insensitive to  $K_D$  values. One of the purposes of this study was to ascertain the effect of  $K_D$  perturbations on TMDD model-predicted outcomes.

Sensitivity analysis is widely used in mathematical modeling to determine the influence of parameter values on response variables, which might provide a means for dimension reduction, and to design informative experiments for enabling the accurate estimation of sensitive parameters.<sup>6</sup> The various techniques of sensitivity analysis<sup>7</sup> have been applied to pharmacokinetic systems ranging in complexity from 1-compartment to full physiologically based models.<sup>8–11</sup> The primary objective of this study is to conduct a sensitivity analysis of selected target-mediated pharmacokinetic models, ascertain the effect of parameter variations on model predictions, and identify influential model parameters.

---

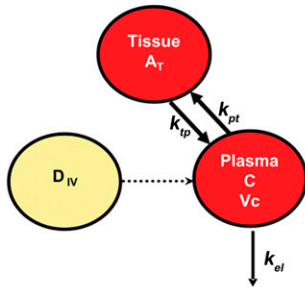
**Corresponding Author:** Donald E. Mager, Department of Pharmaceutical Sciences, University at Buffalo, SUNY, 543 Hochstetter Hall, Buffalo, NY 14260. Tel: (716) 645-2842, ext 277; Fax: (716) 645-3693; E-mail: [dmager@buffalo.edu](mailto:dmager@buffalo.edu)

## METHODS

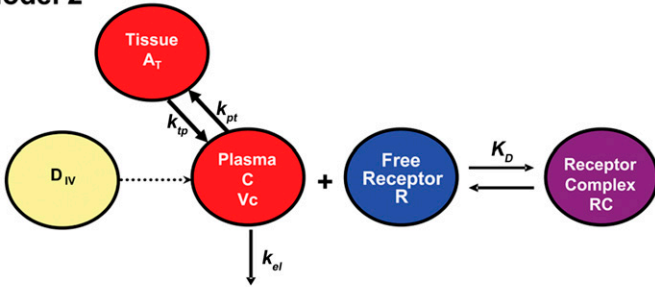
### Structural Models

Three models were selected for analysis: Model 1, a standard 2-compartment linear model; Model 2, a nonlinear model with receptor binding and a constant receptor pool (ie, drug-receptor complex internalization does not occur and there is no receptor turnover); and Model 3, the QEM solution to the general TMDD model (Figure 1). Nominal parameter values and the applicability of each parameter in the above models are listed in Table 1. As shown in Figure 1, Models 1 and 2 are nested versions of the full Model 3. Although any input function may be incorporated into the model structures, only rapid intravenous (IV) injection will be considered. For Model 3, free drug in the central compartment (C) can bind to free receptor (R) and is in rapid equilibrium with the drug-receptor complex (RC). The volume of the central compartment is denoted as  $V_c$ .

#### Model 1



#### Model 2



#### Model 3

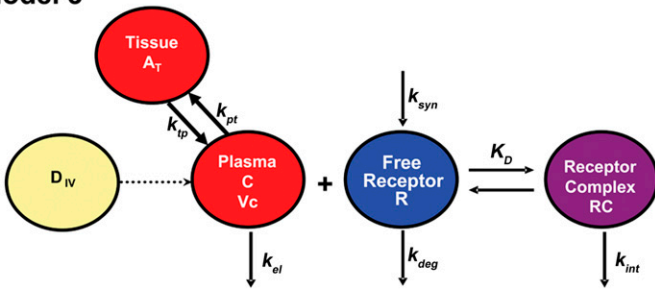


**Figure 1.** Selected structural models. Model 1 is a standard 2-compartment linear model. Model 2 incorporates nonlinear receptor binding, but with no internalization of the drug-receptor complex and no receptor turnover (ie, constant receptor pool). Model 3 is the quasi-equilibrium model, which includes receptor binding and internalization of the drug-receptor complex.

Free drug is also available for elimination from the central compartment by a first-order process ( $k_{el}$ ) as well as non-specific distribution to tissue sites by first-order distribution processes ( $k_{pt}$  and  $k_{tp}$ ). The drug receptor complex may be internalized and is denoted by a first-order rate constant,  $k_{int}$ . The turnover process of free receptor is governed by a zero-order production rate,  $k_{syn}$ , and a first-order degradation rate,  $k_{deg}$ .

The differential equations describing the QEM model are as follows<sup>4</sup>:

$$dC_{tot}/dt = \ln(t) - k_{int} \cdot C_{tot} - (k_{el} + k_{pt} - k_{int}) \cdot C + k_{ip} \cdot A_T / V_c \quad (1)$$

$$dA_T / dt = k_{pt} \cdot C \cdot V_c - k_{tp} \cdot A_T \quad (2)$$

$$dR_{tot} / dt = k_{syn} - (k_{int} - k_{deg}) \cdot (C_{tot} - C) - k_{deg} \cdot R_{tot} \quad (3)$$

where  $C_{tot} = C + RC$  and  $R_{tot} = R + RC$ . The drug concentration in the central compartment is the solution to a quadratic equilibrium equation:

$$C = \frac{1}{2} \left[ (C_{tot} - R_{tot} - K_D) + \sqrt{(C_{tot} - R_{tot} - K_D)^2 + 4 \cdot K_D \cdot C_{tot}} \right] \quad (4)$$

Assuming no prior drug exposure (ie, no endogenous production), the initial conditions for the above system are defined as follows:

$$C_{tot}(0) = \frac{Dose}{V_c}; \quad (5a)$$

$$A_T(0) = 0; \quad (5b)$$

$$R_{tot}(0) = R_0 \quad (5c)$$

The free receptor synthesis rate was calculated from the baseline equation  $k_{syn} = k_{deg} \cdot R_0$ . With no internalization of the receptor complex or turnover of free receptors, Model 3 simplifies to 1 of several nonlinear pharmacokinetic models originally described by Wagner (Model 2).<sup>12</sup>

### Derivation of $\lambda_z$ for Model 3

By definition, the  $\lambda_z$  for the free drug concentration is the negative slope of the terminal part of  $C$  vs  $t$  curve in the semilogarithmic scale:

$$\lambda_z = -\lim_{t \rightarrow \infty} \frac{d \ln(C)}{dt} = -\lim_{t \rightarrow \infty} \frac{1}{C} \frac{dC}{dt} \quad (6)$$

To calculate the derivative  $dC/dt$ , we will use the quasi-equilibrium assumption:

$$\frac{R \cdot C}{RC} = \frac{(R_{tot} - C_{tot} + C)C}{C_{tot} - C} = K_D \quad (7)$$

**Table 1.** Base Model Parameter Values\*

Parameter	Abbreviation	Units	Base Value	Applicable Model(s)
First-order elimination rate constant	$k_{el}$	1/hr	1.49	1, 2, 3
Central volume	$V_c$	mL/kg	51.2	1, 2, 3
First-order tissue distribution rate constants	$k_{pt}, k_{ip}$	1/hr	0.389	1, 2, 3
Equilibrium dissociation rate constant	$K_D$	nM	1.22	2, 3
Initial receptor concentration	$R_0$	nM	8.19	2, 3
Receptor complex internalization rate constant	$k_{int}$	1/hr	3.16	3
Receptor degradation rate constant	$k_{deg}$	1/hr	0.67	3

\*Values are from Mager and Krzyzanski.<sup>4</sup>

After multiplying both sides of Equation 7 by  $(C_{tot} - C)$  and differentiating with respect to time, we obtain Equation 8:

$$\frac{dC}{dt}(R_{tot} - C_{tot} + 2C + K_D) = -C \left( \frac{dR_{tot}}{dt} - \frac{dC_{tot}}{dt} \right) + K_D \frac{dC_{tot}}{dt} \quad (8)$$

Consequently,

$$-\frac{1}{C} \frac{dC}{dt} = \frac{\left( \frac{dR_{tot}}{dt} - \frac{dC_{tot}}{dt} \right)}{(R_{tot} - C_{tot} + 2C + K_D)} - \frac{K_D \frac{1}{C} \cdot \frac{dC_{tot}}{dt}}{(R_{tot} - C_{tot} + 2C + K_D)} \quad (9)$$

For large amounts of time,  $R_{tot}$  and  $C_{tot}$  approach their steady states:

$$R_{tot} \rightarrow R_0 \text{ and } C_{tot} \rightarrow 0 \text{ as } t \rightarrow \infty \quad (10)$$

Therefore,

$$\frac{dR_{tot}}{dt} \rightarrow 0 \text{ and } \frac{dC_{tot}}{dt} \rightarrow 0 \text{ as } t \rightarrow \infty \quad (11)$$

Applying Equations 10 and 11 to Equation 9, we obtain Equation 12:

$$\lambda_z = \frac{K_D}{K_D + R_0} \lim_{t \rightarrow \infty} \frac{1}{C} \frac{dC_{tot}}{dt} \quad (12)$$

To calculate the limit in Equation 12, we can divide Equation 1 by  $C$  and let  $t \rightarrow \infty$ :

$$\lim_{t \rightarrow \infty} \frac{1}{C} \frac{dC_{tot}}{dt} = -k_{int} \cdot X - (k_{el} + k_{pt} - k_{int}) + k_{ip} \cdot y \quad (13)$$

where

$$x = \lim_{t \rightarrow \infty} \frac{C_{tot}}{C} \text{ and,} \quad (14a)$$

$$y = \lim_{t \rightarrow \infty} \frac{A_T/V_c}{C} \quad (14b)$$

L'Hospital's rule states:

$$x = -\frac{1}{\lambda_z} \lim_{t \rightarrow \infty} \frac{1}{C} \frac{dC_{tot}}{dt} \text{ and,} \quad (15a)$$

$$y = -\frac{1}{\lambda_z \cdot V_c} \lim_{t \rightarrow \infty} \frac{1}{C} \frac{dA_T}{dt} \quad (15b)$$

Equations 15a and 13 imply that

$$-\lambda_z \cdot x = -k_{int} \cdot x - (k_{el} + k_{pt} - k_{int}) + k_{ip} \cdot y \quad (16)$$

and Equations 15b and 2 yield

$$-\lambda_z \cdot y = k_{pt} - k_{ip} \cdot y \quad (17)$$

Solving Equations 16 and 17 for x results in

$$x = \frac{\lambda_z(k_{el} + k_{pt} - k_{int}) - k_{ip}(k_{el} - k_{int})}{(\lambda_z - k_{int})(\lambda_z - k_{pt})} \quad (18)$$

Equations 15a and 12 imply that

$$1 = \frac{K_D x}{K_D + R_0} \quad (19)$$

Equations 18 and 19 can be combined to obtain

$$\lambda_z^2 - \frac{(k_{int} + k_{ip})R_0 + K_D(k_{el} + k_{ip} + k_{pt})}{K_D + R_0} \lambda_z + \frac{k_{ip}(k_{int}R_0 + K_D k_{el})}{K_D + R_0} = 0 \quad (20)$$

Hence, the smallest positive solution is

$$\lambda_z = \frac{1}{2} \left( k_{ip} + \frac{k_{int}R_0 + K_D(k_{el} + k_{pt})}{K_D + R_0} \right) - \frac{1}{2} \sqrt{\left( k_{ip} + \frac{k_{int}R_0 + K_D(k_{el} + k_{pt})}{K_D + R_0} \right)^2 - 4k_{ip} \frac{k_{int}R_0 + K_D k_{el}}{K_D + R_0}} \quad (21)$$

### Sensitivity Analysis

As part of a preliminary analysis, a one-at-a-time sensitivity measure/analysis approach was adopted.<sup>13</sup> The partial derivative of model output with respect to the perturbed parameter provides a measure of the model sensitivity to each parameter. Nominal parameter values were taken from the previous analysis of LIF pharmacokinetic data.<sup>4</sup>

IV bolus doses for the simulation, obtained from the dose-ranging study of LIF in sheep, are 12.5, 25, 100, 250, 500, and 750  $\mu\text{g}/\text{kg}$ .<sup>5</sup> A generic model code was written in WinNonlin (Pro V 4.1, Pharsight, Mountain View, CA), allowing for log-fold alterations in parameter values and/or transition between the different models by setting parameters that are not applicable to a model to the null value. In addition to the transition between the different models, the code could be used to account for endogenous production of the molecule, as necessary. For Model 1, the parameters  $k_{\text{int}}$ ,  $k_{\text{deg}}$ , and  $R_0$  from Model 3 were set to zero, which in effect reduced the QEM model to a simple 2-compartment model. Model 2 accounts for receptor binding; parameters  $k_{\text{deg}}$  and  $k_{\text{int}}$  were set to zero. The resultant model is a 2-compartment model with rapid nonlinear binding in the central compartment and a constant receptor pool.<sup>12</sup>

A series of simulations were conducted with differing parameter values, which were varied 10-, 100-, and 1000-fold on the lower and higher side of the LIF base value.<sup>5</sup> Each simulation was conducted by altering 1 parameter at a time and fixing all remaining parameter values. All simulations were performed using WinNonlin. The outputs considered for the subsequent parameter sensitivity analysis were the simulated concentration-time profiles and partial derivative plots of concentration with respect to the altered parameter. The 250  $\mu\text{g}/\text{kg}$  dose was selected for parameter perturbations, as this intermediate dose encompassed the linear as well the transient nonlinear receptor saturation phase. Profiles were generated up to a 25-hour time point, with 501 observations per run. The parameter perturbations are in the log-fold range and may not be physiologically relevant. However, the purpose of the analysis was to test the sensitivity of the model by subjecting it to extreme parametric value perturbations and to ascertain which parameters influence the model output. In addition, partial derivatives for each parameter at the nominal value were normalized to the parameter and concentration for each time point:  $\partial C/\partial P \times P/C$ , where  $P$  is the parameter of interest. Such normalized sensitivity coefficients may be used to assess the relative sensitivity of concentrations (or system output) across model parameters.<sup>7</sup>

### RESULTS AND DISCUSSION

The simulated concentration-time profiles for the different dose levels are provided in Figure 2. As expected, the resultant pharmacokinetic profile from Model 1 is biexponential and the terminal phase is parallel for each dose.

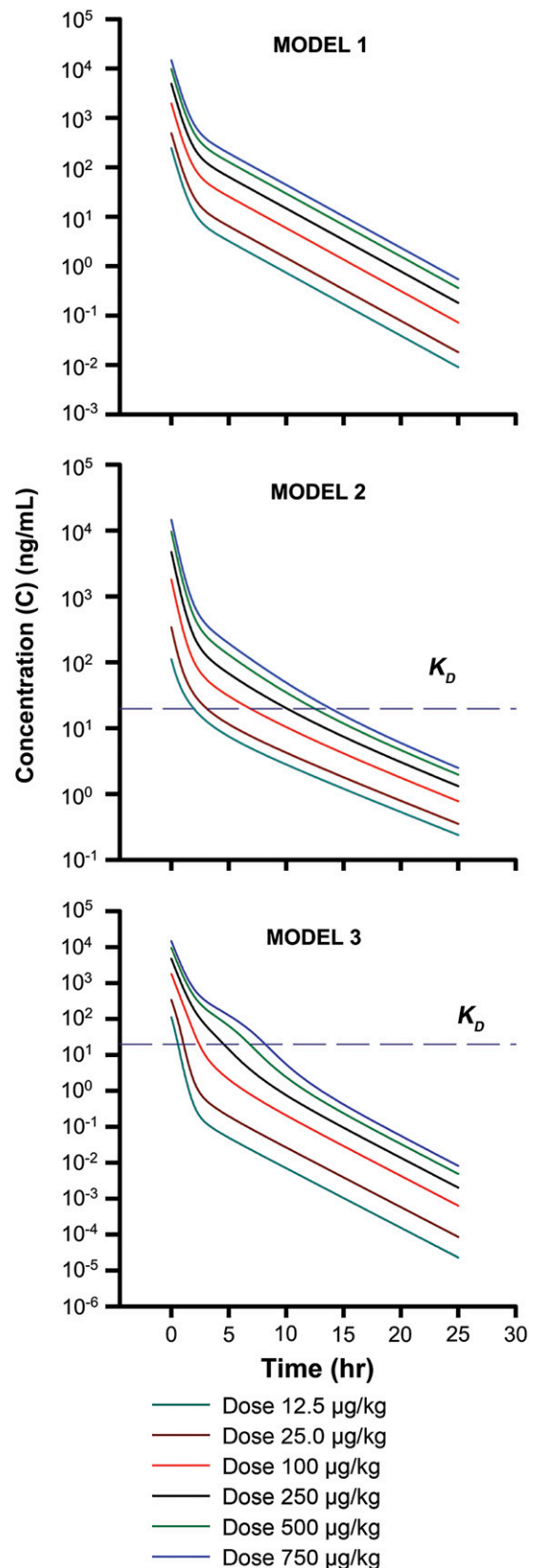


**Figure 2.** Dose-ranging simulation of free drug concentration-time profiles for each model. Simulations for the 12.5, 25.0, 100, 250, 500, and 750  $\mu\text{g}/\text{kg}$  doses for each model are shown. The horizontal broken line in the middle and bottom panels denotes the  $K_D$  value (1.22 nM) of the drug (Models 2 and 3). Model parameters used for the simulations are presented in Table 1.

Model 2 incorporates receptor binding, and profiles indicate a subtle triphasic profile for drug concentrations above the  $K_D$  value, which is attributed to the nonlinear receptor saturation phase. The terminal phase for each dose is parallel at earlier times but is expected to converge at later times.<sup>2</sup> Model 3 is characterized by a rapid initial drop, followed by the intermediate nonlinear receptor saturation phase, which is clearly seen for the 250, 500, and 750  $\mu\text{g}/\text{kg}$  dose levels.

Simulated free receptor profiles for Models 2 and 3 are shown in Figure 3. Profiles for Model 2 are consistent with basic expectations from the respective concentration-time profiles for each dose level. The free receptor concentration shows a rapid drop, as a result of receptor binding for the high ligand concentration at earlier times. For higher doses, the concentration of the free receptor remains at the plateau for longer times, until free ligand is slowly eliminated from the system relative to the  $K_D$  value. Free receptor concentration eventually returns to baseline levels after complete elimination of the ligand, with an expected right shift for increasing dose levels. In Model 3, the initial drop is similar to Model 2's; however, the return to baseline is much more gradual for the higher dose levels. This is the result of a complex interplay between elimination, drug-receptor internalization, and receptor turnover.

Whereas total receptor concentration ( $R_{tot}$ ) for Model 2 remains constant, the total receptor profile for Model 3 (Figure 4) plateaus at a lower limiting value for higher dose levels before gradually returning to baseline. The concentration of  $R_{tot}$  does not reach a limiting value of zero, owing to the receptor turnover process. The return of total receptors to baseline is explained by an increase in the free receptor as drug is eliminated from the system.

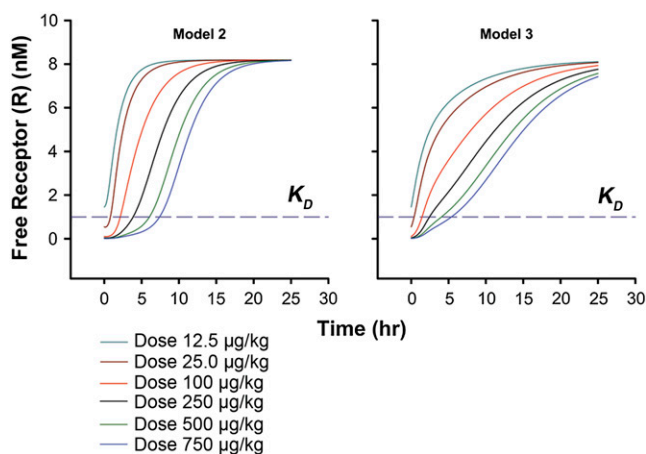


**Figure 3.** Dose-ranging simulation of free receptor-time profiles for Models 2 and 3. The horizontal broken line for both model simulations denotes the  $K_D$  value (1.22 nM) of the drug. Model parameters used for the simulations are presented in Table 1.

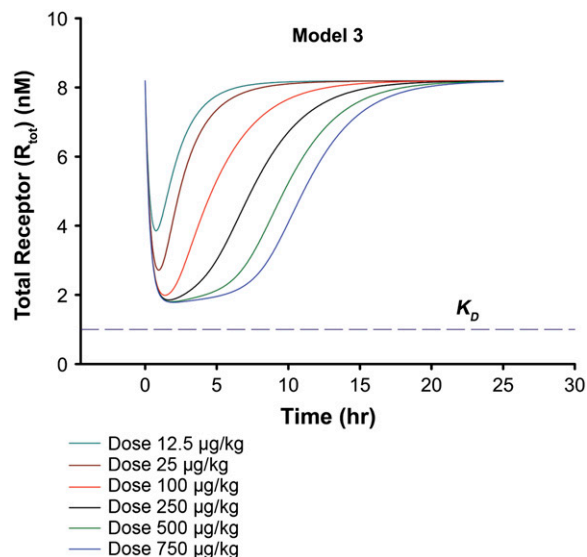


**Figure 4.** Dose-ranging simulation of total receptor-time profiles for Model 3. The horizontal broken line in the graph denotes the  $K_D$  value (1.22 nM) of the drug. Model parameters used for the simulations are presented in Table 1.

### Sensitivity Analysis

The model outputs were found to be highly sensitive to parameter perturbations of linear drug disposition ( $k_{el}$ ,  $V_c$ ,  $k_{pb}$  and  $k_{ip}$ ) for each of the 3 models (data not shown). Given the focus of this study on the sensitivity of model output to perturbations in parameters associated with nonlinear binding ( $K_D$ ,  $R_0$ ,  $k_{int}$ , and  $k_{deg}$ ) and the fact that Model 1 does not incorporate nonlinear binding, further discussion will be limited to the evaluation of outputs for the nonlinear system parameters of Models 2 and 3.

Model outcomes following variations in  $K_D$  are shown in Figure 5A. The perturbations at the lower end of the base parameter values are denoted by the letter L and at the higher end by the letter G. The fold variations are denoted by numerals corresponding to the extent of variation. For example, L1000 would be a 1000-fold change in the parameter at the lower end from the base value of the parameter. Simulations were performed to 100 hours for Model 2, because of the incomplete resolution of model output obtained up to 25 hours. The concentration profiles seem to deviate from each other at later times for lower values of  $K_D$ . The terminal slope ( $\lambda_z$ ) for Model 2 in the absence of tissue distribution is given as<sup>12</sup>

$$\lambda_z = \frac{k_{el}}{1 + \frac{R_{tot}}{K_D}} \quad (22)$$

For extreme values of  $K_D$ , the  $\lambda_z$  approaches a limiting value. For very high values ( $K_D \rightarrow \infty$ ),  $\lambda_z$  approaches  $k_{el}$ , and for very low values, the  $\lambda_z$  approaches 0. One may visualize the system, wherein for a high  $K_D$  the drug is essentially

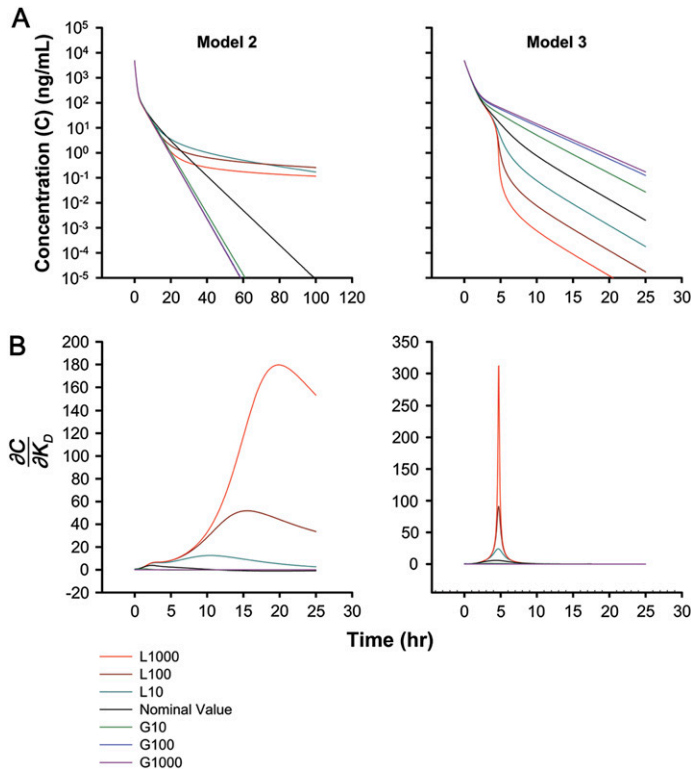


**Figure 5.** (A) Simulated drug concentration-time profiles for perturbations in  $K_D$  at the 250  $\mu\text{g}/\text{kg}$  dose level. The values were perturbed 10-, 100-, and 1000-fold at the higher and lower ends of the base value of  $K_D$ . (B) Partial derivative plot for perturbations in the base value of  $K_D$ .

unbound (ie, the effect of binding is negligible) and for a low  $K_D$  the drug does not dissociate from the receptor rapidly. At the extremes, the system essentially approaches linearity and is relatively insensitive to variations in  $K_D$ . Inclusion of a tissue compartment ( $k_{pt} > 0$ ,  $k_{ip} > 0$ ) influences the terminal slope such that

$$\lambda_z = \frac{1}{2} \left( k_{ip} + \frac{K_D(k_{el} + k_{pt})}{K_D + R_0} \right) - \frac{1}{2} \sqrt{\left( k_{ip} + \frac{K_D(k_{el} + k_{pt})}{K_D + R_0} \right)^2 - 4k_{ip} \frac{K_D k_{el}}{K_D + R_0}} \quad (23)$$

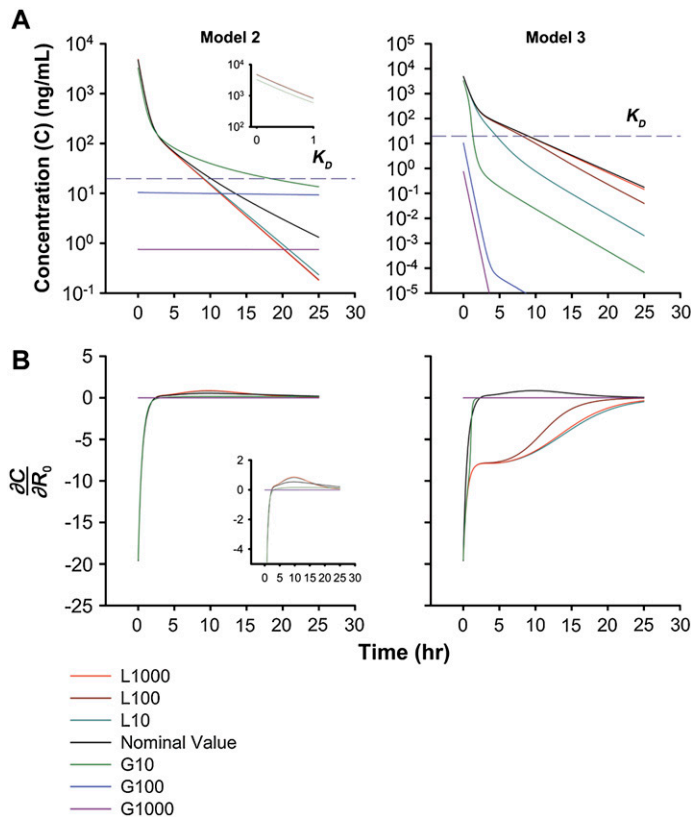
which derives from setting  $k_{int} = 0$  in the equation for the terminal slope of Model 3 (see Equation 21). The inflection point for each of the  $K_D$ -varied curves coincides with the peaks obtained from the partial derivative curve (Figure 5B). One may argue that in order to accurately estimate the parameter  $K_D$ , one must have measurements at later times coinciding with the partial derivative peaks. This might be complicated by the assay limit of quantification, and a sensitive assay would be required to detect the drug at later times.

The terminal slope for Model 3 is defined by the full Equation 21 ( $k_{pt} > 0$ ,  $k_{ip} > 0$ ). It is evident from the equation that the terminal slope of the concentration-time profiles for Model 3 is a complicated function of the system parameters. For high and low values of  $K_D$ , the terminal slopes appear to be parallel. Thus, the concentration output is relatively sensitive to changes in  $K_D$  at the lower end of the perturbations. The inflection point for all values of  $K_D$  occurs at the 5-hour time point. The partial derivative plots confirm that the maximum information about  $K_D$  is obtained at this time point for Model 3 (for the selected dose), as concentrations approach the  $K_D$  value. The time point would be expected to shift depending on the chosen dose level.

Simulated outcomes for perturbations in the initial receptor concentration ( $R_0$ ) are provided in Figure 6. The initial drug concentration ( $C_0$ ) differs for variations in the  $R_0$  value. An increase in the initial receptor concentration at a given  $K_D$  results in an increase in the amount of bound drug and an immediate drop in the free concentration of the drug. The extent of the decrease in  $C_0$  is controlled by the magnitude of the initial concentration of free receptor. Likewise, a low initial receptor concentration for Model 2 results in a higher initial drug concentration. Figure 6A shows differences in  $C_0$  values for perturbations in  $R_0$  and is evident at the higher end of parameter perturbations. The resultant output due to changes in parameter  $R_0$  parallels the changes seen with perturbations in the volume of distribution (data not shown). Free drug is rapidly acquired by free receptor, thus effectively reducing the initial free concentration of the drug in the central compartment. For Model 3, the degradation of the free receptor and internalization of the drug-receptor complex offsets this rapid drop in free drug concentrations for higher-end variations of  $R_0$ , as shown for Model 2. The initial drop is less steep, with a clearly discernible  $\alpha$  phase.

Models 2 and 3 are both sensitive to the parameter for variations at the higher end of parameter perturbation. Model 3 is most sensitive to nonlinear receptor binding in the  $\alpha$  phase. With reference to the partial derivatives, it is evident that the maximum information about  $R_0$  is at early time points. From a study design perspective, it is often difficult to obtain blood samples so soon after drug administration.

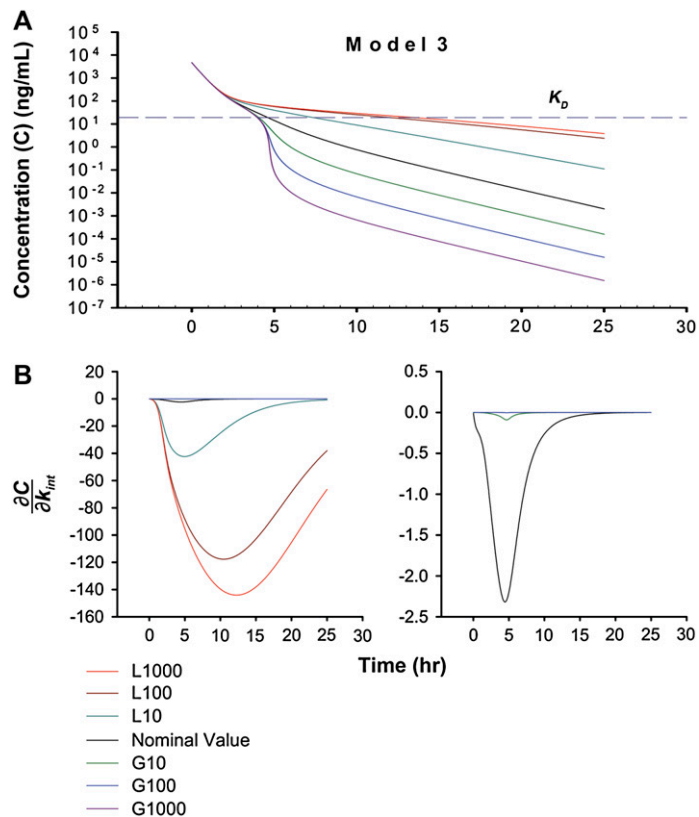
Model 3 includes important parameters related to receptor turnover and receptor-complex internalization processes ( $k_{int}$  and  $k_{deg}$ ). Equation 21 implies that the terminal slope variations are influenced by changes in  $k_{int}$  as well as changes in  $K_D$ . Simulated profiles following perturbations of  $k_{int}$  are shown in Figure 7. As expected, no change was observed for the model predictions at earlier times when the free concentrations were above the  $K_D$ . The convex inflection point of the concentration profiles for all perturbations of  $k_{int}$ , except L100 and L1000, occur at roughly



**Figure 6.** (A) Simulated drug concentration-time profiles for perturbations in  $R_0$  at the 250 µg/kg dose level. The values were perturbed 10-, 100-, and 1000-fold at the higher and lower ends of the base value of  $R_0$ . Inset figure for Model 2 shows that perturbations in the initial receptor concentrations result in differing initial drug concentrations. (B) Partial derivative plot for perturbations in the base value for  $R_0$ . Inset figure for Model 2 shows the partial derivative plots at early time points.

the 5-hour time point, as concentrations approach the  $K_D$  value. The divergence of the profiles at later times can be explained by considering  $k_{int} \rightarrow 0$ , where the terminal slope is essentially constant and is determined by the values of the remaining parametric terms. Equation 21 contains the  $k_{int}$  parameter in the numerator; as a result, for increasing values of  $k_{int}$  the profiles tend to diverge at later times. The magnitude of the divergence is dependent on the extent of the perturbation of  $k_{int}$  for values in the ascending order. The greater the value of  $k_{int}$ , the greater the value of  $\lambda_z$ .

The partial derivatives for all variations of  $k_{int}$  (Figure 7B), with the exception of L100 and L1000, result in a peak at 5 hours. Sampling at the 5-hour time point again seems to be crucial for the chosen dose level. The partial derivative plots for the L100 and L1000 perturbations of  $k_{int}$  necessitate the incorporation of a sampling beyond 5 hours, perhaps because the concentration approaches the  $K_D$  at these later time points.



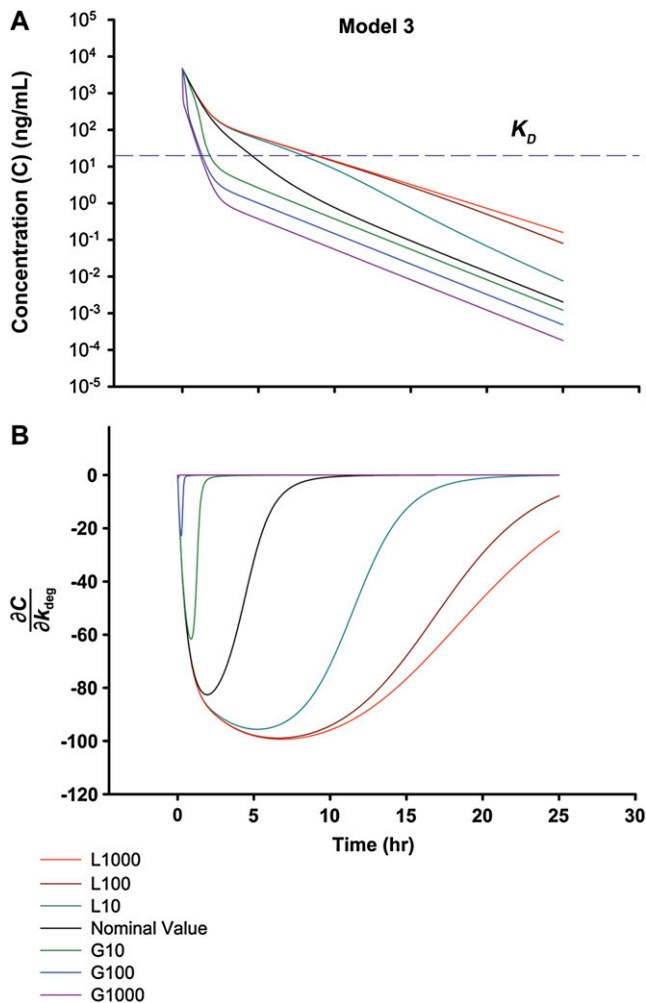
**Figure 7.** (A) Simulated drug concentration-time profiles for perturbations in  $k_{int}$  at the 250 µg/kg dose level. The values were perturbed 10-, 100-, and 1000-fold at the higher and lower ends of the base value of  $k_{int}$ . (B) Partial derivative plot for perturbations in the base value of  $k_{int}$ . The panel at the bottom right shows the partial derivative plot at early time points.

Figure 8 includes simulations relevant to variations in  $k_{deg}$ . The smallest positive solution of Equation 21 for  $\lambda_z$ , as  $k_{deg} \rightarrow \infty$  and  $R_0 \rightarrow 0$ , is as follows:

$$\lambda_z = \frac{1}{2} \left[ (k_p + k_{el} + k_{pt}) - \sqrt{(k_p + k_{el} + k_{pt})^2 - 4 \cdot k_p \cdot k_{el}} \right] \quad (24)$$

The parallel terminal slopes observed for the higher-end variations of  $k_{deg}$  have a limiting value given by Equation 24, and the inflection point for each variation is independent of  $K_D$ . The lower-end variations were relatively insensitive in the initial phase of decline, and the inflection point for these variations occurs when free concentrations approach the  $K_D$  value. Also, increasing the receptor degradation rate constant resulted in an overall decreased exposure to free drug. For concentrations above the  $K_D$ , the model is sensitive to variations of  $k_{deg}$  at the higher end of the parameter space.

Finally, whereas local sensitivity analysis reveals sampling points where maximum information about each parameter may be obtained and illustrates certain dynamic properties of the structural model, normalized sensitivity indices provide a means for ascertaining the relative sensitivity across



**Figure 8.** (A) Simulated drug concentration-time profiles for perturbations in  $k_{deg}$  at the 250 µg/kg dose level. The values were perturbed 10-, 100-, and 1000-fold at the higher and lower ends of the base value of  $k_{deg}$ . (B) Partial derivative plot for perturbations in the base value of  $k_{deg}$ .

parameters and may add insight into the overall behavior of the system.<sup>7</sup> The computed values of the sensitivity coefficients for each parameter are provided in Table 2. Model 2 is relatively insensitive at earlier times for perturbations in  $K_D$  and  $R_0$ , although maximum information for these parameters is obtained at earlier times (Figures 5B and 6B). The model is highly sensitive at later times, with  $K_D$  exhibiting a greater influence compared with  $R_0$ . For Model 3, the output is sensitive at 5 hours for  $K_D$ , and at later times, the model sensitivity is high for both  $K_D$  and  $R_0$ . Additionally,  $k_{int}$  influenced model output the most at later times and  $k_{deg}$  was least influential at 25 hours. For nonlinear models, a local sensitivity analysis does not provide conclusive results. Further studies should be conducted using a global sensitivity approach, wherein multiple parameters are changed simultaneously.<sup>14</sup> Such an approach will allow an assessment of parameter interactions, if any, within each model.

**Table 2.** Normalized Partial Derivatives (Sensitivity Coefficients)

Parameter	Model 2		Model 3	
	5 Hours	25 Hours	5 Hours	25 Hours
$K_D$	0.0424	1.74	0.454	1.10
$R_0$	0.0424	1.21	0.0575	2.61
$k_{int}$	—	—	-1.26	-3.24
$k_{deg}$	—	—	-1.51	-0.249

## CONCLUSION

Selected TMDD models subjected to parameter perturbations were evaluated to gain a better understanding of model behavior. Local sensitivity analysis allowed the elucidation of model outcomes with respect to each parameter. All models were sensitive to perturbations in standard parameters of linear disposition. The influence of  $K_D$  in the terminal phase for Model 3 necessitates sample measurements at later time points, and the relevance of early time points for accurate estimation of  $R_0$  has been demonstrated. Thus, as highlighted in this study, informed study designs of TMDD systems may be of critical importance for the accurate estimation of influential model parameters.

## ACKNOWLEDGMENTS

This study was supported in part by funds from Grant 57980 (for W. Krzyzanski and D. E. Mager) from the National Institutes of Health; startup funds (to D. E. Mager) from the University at Buffalo, State University of New York; and funds from the University at Buffalo–Pfizer Strategic Alliance (for A. Abraham).

## REFERENCES

- Levy G. Pharmacologic target-mediated drug disposition. *Clin Pharmacol Ther.* 1994;56:248-252.
- Mager DE, Jusko WJ. General pharmacokinetic model for drugs exhibiting target-mediated drug disposition. *J Pharmacokinet Pharmacodyn.* 2001;28:507-532.
- Mager DE. Target-mediated drug disposition and dynamics. *Biochem Pharmacol.* 2006;72:1-10.
- Mager D, Krzyzanski W. Quasi-equilibrium pharmacokinetic model for drugs exhibiting target-mediated drug disposition. *Pharm Res.* 2005;22:1589-1596.
- Segrave AM, Mager DE, Charman SA, Edwards GA, Porter CJ. Pharmacokinetics of recombinant human leukemia inhibitory factor in sheep. *J Pharmacol Exp Ther.* 2004;309:1085-1092.
- Varkonyi P, Bruckner JV, Gallo JM. Effect of parameter variability on physiologically-based pharmacokinetic model predicted drug concentrations. *J Pharm Sci.* 1995;84:381-384.



7. Hamby DM. A review of techniques for parameter sensitivity analysis of environmental models. *Environ Monit Assess.* 1994;32:135-154.
8. Wu G. Sensitivity analysis of pharmacokinetic parameters in one-compartment models. *Pharmacol Res.* 2000;41:445-453.
9. Nestorov IA. Sensitivity analysis of pharmacokinetic and pharmacodynamic systems, I: a structural approach to sensitivity analysis of physiologically based pharmacokinetic models. *J Pharmacokinet Biopharm.* 1999;27:577-596.
10. Nestorov IA, Aarons LJ, Rowland M. Physiologically based pharmacokinetic modeling of a homologous series of barbiturates in the rat: a sensitivity analysis. *J Pharmacokinet Biopharm.* 1997;25:413-447.
11. Hetrick DM, Jarabek AM, Travis CC. Sensitivity analysis for physiologically based pharmacokinetic models. *J Pharmacokinet Biopharm.* 1991;19:1-20.
12. Wagner JG. A new generalized nonlinear pharmacokinetic model and its implications. In: Wagner JG, ed. *Biopharmaceutics and Relevant Pharmacokinetics*. Hamilton, IL: Drug Intelligence Publications; 1971:302-317.
13. Hamby DM. A comparison of sensitivity analysis techniques. *Health Phys.* 1995;68:195-204.
14. Saltelli A, Tarantola S, Chan KPS. A quantitative model-independent method for global sensitivity analysis of model output. *Technometrics.* 1999;41:39-56.